Available online at www.sciencedirect.com
SCIENCE DIRECT®
European Journal of Mechanics B/Fluids 25 (2006) 74–82

The convective stability of circular Couette flow induced by a linearly accelerated inner cylinder

Min Chan Kim [a,*], Sin Kim [b], Chang Kyun Choi [c]

[a] *Department of Chemical Engineering, Cheju National University, Cheju 690-756, Republic of Korea*
[b] *Department of Nuclear and Energy Engineering, Cheju National University, Cheju 690-756, Republic of Korea*
[c] *School of Chemical Engineering, Seoul National University, Seoul 151-744, Republic of Korea*

Received 4 December 2003; received in revised form 19 October 2004; accepted 21 April 2005

Available online 23 June 2005

Abstract

The onset of Taylor–Görtler instability induced by a linearly accelerated inner cylinder in Couette flow is analyzed by using the propagation theory based on linear theory and momentary instability concept. It is well-known that the primary transient Couette flow is laminar but secondary motion sets in when the inner cylinder velocity exceeds a certain value. The dimensionless critical time τ_c to mark the onset of instability is presented here as a function of the modified Taylor number T. Available experimental data indicate that for large T secondary motion is detected starting from a certain time $\tau \approx 2\tau_c$. This means that the growth period of initiated instabilities is needed for secondary motion to be detected experimentally. It seems evident that during $\tau_c \leqslant \tau \leqslant 2\tau_c$ secondary motion is relatively very weak and the primary diffusive momentum transfer is dominant.

Keywords: Taylor–Görtler vortex; Couette flow; Linear acceleration; Hydrodynamic instability; Propagation theory

1. Introduction

It is well-known that in the primary laminar flows along concavely curved walls the destabilizing action of centrifugal forces can produce secondary motion in form of vortices. The related hydrodynamic instabilities usually lead to Taylor vortices in the flow between rotating concentric cylinders or Görtler vortices in the boundary layer flow. This kind of secondary flow occurs in the wide range of scientific and engineering fields [1,2]. Most of real situations involve nonlinear and developing basic velocity profiles and therefore the critical time or the critical position to mark the onset of secondary motion becomes an important question.

The instability problem of transient Couette flow in a cylinder is closely related with that of Taylor–Görtler vortices. The onset of instability caused by the centrifugal forces in circular Couette flow was investigated experimentally by Chen and Christensen [3] for the impulsively accelerated system and Chen et al. [4] for the linearly accelerated system. The initial laminar flow evolves into a secondary flow pattern which consists of a series of Taylor-like vortices. The related stability problem has been analyzed theoretically by the frozen-time model [5], the amplification theory [4,5], the energy method [6], the maximum-Taylor-number criterion [7] and the propagation theory [8–10]. MacKerrell et al. [11] delineated the stability region based on

* Corresponding author. Tel.: +82 64 754 3685; fax: +82 64 755 3670.
E-mail address: mckim@cheju.ac.kr (M.C. Kim).

0997-7546/$ – see front matter
doi:10.1016/j.euromechflu.2005.04.009

the frozen-time model for the various accelerating cases. These models are closely related with Rayleigh–Bénard problems. The frozen-time model is based on linear theory and yields the critical time as the parameter. The amplification theory requires the initial conditions and the criterion to define detection of manifest convection. The energy method yields lower bounds on experimental detection times. The amplification theory and the energy method are quite popular, but they require a large number of computations. Even though the maximum-Taylor-number criterion is the simplest one, it seems to be in lack of physical insights. The propagation theory assumes that at time $t = t_c$ infinitesimal angular velocity disturbances are propagated mainly within the boundary-layer thickness and with this length scaling factor all the variables and parameters having the length scale are rescaled.

Here we will extend the propagation theory, which has been employed to analyze time-dependent Rayleigh–Bénard problems, to the hydrodynamic instability induced by a linearly accelerated inner cylinder in Couette flow. The effect of a finite acceleration on the onset time of secondary motion and also the wavelength will be examined and the resulting predictions will be discussed in comparison with available experimental and theoretical results.

2. Theoretical analysis

2.1. Governing equations

The system considered here is a Newtonian fluid confined between two concentric cylinders of radii R_i and R_o. Let the axis of the cylinders be along the vertical z'-axis under the cylindrical coordinates (r', θ, z') and the corresponding velocities be U, V and W. Initially, the entire fluid/cylinder system is kept at quiescent state. Starting from time $t = 0$, the inner cylinder is accelerated with a constant acceleration rate A. The schematic diagram of the present system is shown in Fig. 1. This flow encounters instabilities in form of Taylor–Görtler vortices and the governing equations of the flow field are expressed as

$$\nabla \cdot \mathbf{U} = 0, \tag{1}$$

$$\left\{\frac{\partial}{\partial t} + \mathbf{U}\cdot\nabla\right\}\mathbf{U} = -\frac{1}{\rho}\nabla P + \nu\nabla^2\mathbf{U}, \tag{2}$$

where $\mathbf{U}$ $(= \mathbf{e}_r U + \mathbf{e}_\theta V + \mathbf{e}_z W)$, P, ν, ρ, and $\mathbf{e}_i$ represent the velocity vector, the dynamic pressure, the kinematic viscosity, the density, and the unit vector at the i-direction, respectively.

For the case of constant physical properties the primary-velocity field is represented:

$$\frac{\partial V_0}{\partial t} = \nu D' D'_* V_0, \tag{3}$$

with the following initial and boundary conditions,

$$V_0 = 0 \quad \text{for } t \leqslant 0, \tag{4a}$$

$$V_0 = At \quad \text{at } r' = R_i \text{ for } t > 0, \tag{4b}$$

$$V_0 = 0 \quad \text{at } r' = R_o \text{ for } t > 0, \tag{4c}$$

where $D' = \partial/\partial r'$, $D'_* = D' + 1/r'$ and the subscript '0' means the basic quantity. By applying Duhamel's superposition integral to Chen and Kirchner's [5] solution for the impulsively accelerating case, the analytical and exact solution can be obtained as

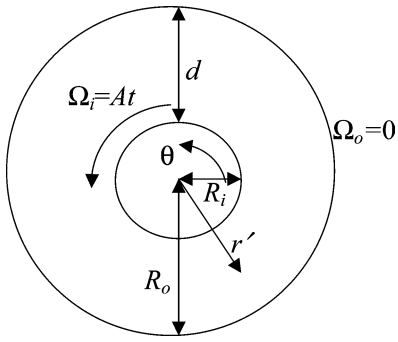

Fig. 1. Top view of the basic system considered here.

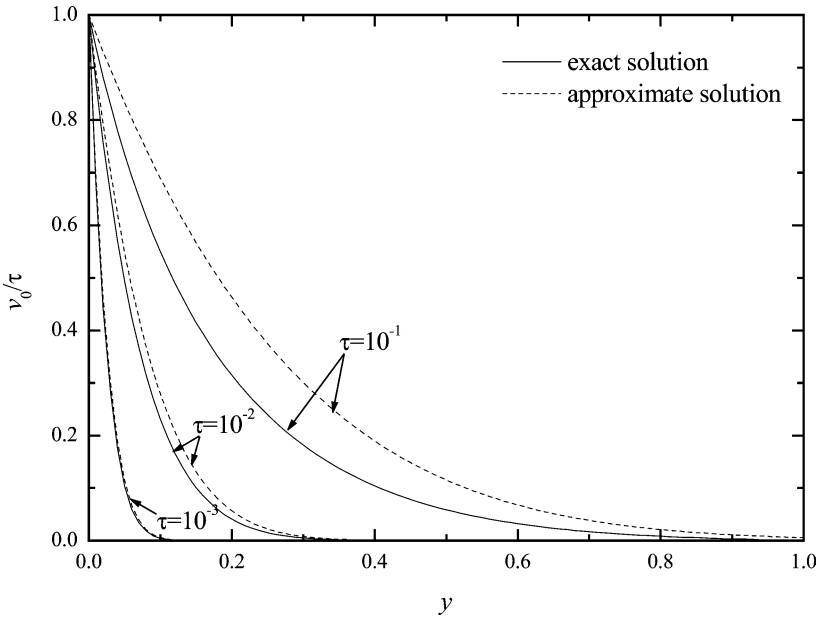

Fig. 2. Primary-velocity profiles for $\eta = 0.2$.

$$v_0(\tau, x) = \frac{\eta}{\xi}\left(\frac{\xi^2 - 1}{\eta^2 - 1}\right) + \sum_{i=0}^{\infty} Q(\beta_i, \eta)\left[J_1\left(\beta_i \frac{\xi}{\eta}\right)Y_1(\beta_i) - J_1(\beta_i)Y_1\left(\beta_i \frac{\xi}{\eta}\right)\right]\frac{1 - \exp\{-\beta_i^2 \eta^2 \tau/(1-\eta)^2\}}{\beta_i^2}, \tag{5a}$$

$$Q(\lambda_i, \eta) = \frac{\eta^2}{(1-\eta)^2}\frac{\pi}{\{[J_1(\beta_i)/J_1(\beta_i/\eta)]^2 - 1\}}, \tag{5b}$$

$$\frac{\xi}{\eta} = \frac{1+\eta}{2\eta} + \frac{1-\eta}{\eta}x, \tag{5c}$$

where $v_0 = V_0/V_r$, $V_r = (Ad^2)/\nu$, $\eta = R_\mathrm{i}/R_\mathrm{o}$, $x = \{(r' - R_\mathrm{i}) + (r' - R_\mathrm{o})\}/2d$, $d = R_\mathrm{o} - R_\mathrm{i}$ and $\tau = \nu t/d^2$. Here J_1 and Y_1 denote the first order Bessel functions of the first and second kind and the β_i's are the roots of

$$J_1\left(\frac{\beta_i}{\eta}\right)Y_1(\beta_i) - J_1(\beta_i)Y_1\left(\frac{\beta_i}{\eta}\right) = 0. \tag{5d}$$

For the deep-pool region of extremely small time, the above velocity profile reduces to

$$v_0 = 4\tau \mathrm{i}^2\,\mathrm{erfc}\left[\frac{y}{\sqrt{4\tau}}\right], \tag{6}$$

where $y = (r' - R_\mathrm{i})/d$ and

$$\mathrm{i}^2\,\mathrm{erfc}(\xi) = \frac{1}{4}\left[(1 + 2\xi^2)\,\mathrm{erfc}(\xi) - \frac{2}{\sqrt{\pi}}\xi \exp(-\xi^2)\right].$$

For $\eta = 0.2$ the above solutions are compared with the exact ones in Fig. 2. For $\tau = 10^{-3}$ Eq. (6) is almost exact, as shown in the figure. With increasing η but decreasing τ it approaches Eq. (5). Since the present study concerns deep-pool systems of small time, Eq. (6) will be used in the stability analysis. The problem is to find the dimensionless critical time τ_c to mark the onset of instability, which grows with time.

2.2. Stability equations

The axisymmetric disturbances which are observed experimentally are well represented by

$$(U_1, V_1, P_1) = (u', v', p')\cos kz', \tag{7a}$$

$$W_1 = w' \sin kz', \tag{7b}$$

where k $(=2\pi/\lambda)$ represents the wavenumber and λ is the wavelength of vortex cells. The subscript '1' denotes the disturbance quantity and the primed quantities representing disturbance amplitudes are functions of r' and t. The two-dimensional perturbed quantities are periodic in the z'-direction. Under linear theory the stability equations of amplitude functions are obtained when w' and p' are eliminated from Eqs. (1) and (2):

$$\left(D'D'_* - k^2 - \frac{1}{\nu}\frac{\partial}{\partial t}\right)(D'D'_* - k^2)u' = 2\frac{V_0}{r'}\frac{k^2}{\nu}v', \tag{8}$$

$$\left(D'D'_* - k^2 - \frac{1}{\nu}\frac{\partial}{\partial t}\right)v' = \frac{D'_* V_0}{\nu}u', \tag{9}$$

with no-slip boundary conditions at $r' = R_\mathrm{i}$ and $r' = R_\mathrm{o}$,

$$u' = D'u' = v' = 0 \quad \text{at } r' = R_\mathrm{i} \text{ and } r' = R_\mathrm{o}. \tag{10}$$

The derivation of all the above equations is described in detail by Chandrasekhar [12]. For the deep-pool region of small τ, where $\sqrt{\nu t}/d \ll 1$, the resulting dimensionless amplitude equations are represented by

$$\left(D^2 - a^2 - \frac{\partial}{\partial \tau}\right)(D^2 - a^2)u = v_0 a^2 v, \tag{11}$$

$$\left(D^2 - a^2 - \frac{\partial}{\partial \tau}\right)v = 2TDv_0 u, \tag{12}$$

where $D = \partial/\partial r$, $D^2 = \partial^2/\partial r^2$ and $r = r'/d$. This kind of geometrical simplification is called the narrow gap approximation, where $\partial/\partial r + 1/r \approx \partial/\partial r$ [12]. Here the nondimensional velocity perturbations have been nondimensionalized as $u = \nu u'/(Td)$ and $v = 2v'/V_r$, a is the dimensionless wavenumber $(= kd)$ in the z'-direction, and $T = (Ad^3/\nu^2)^2(d/R_\mathrm{i})$ is the modified Taylor number.

The propagation theory employed to find the onset time of instability, i.e. the critical time t_c, requires the assumption that in deep-pool systems of small time, the perturbed angular velocity component v' is propagated mainly within the boundary-layer thickness $\Delta(\propto \sqrt{\nu t})$ at the onset time of instability, which will be discussed later. From the r'- and θ-component in Eq. (2), the scale relations for disturbance quantities are given by

$$\nu\frac{\partial^2 u'}{\partial r'^2} \sim \nu\frac{u'}{\Delta^2} \sim \frac{V_\mathrm{i}}{r'}v' \sim \frac{V_\mathrm{i}}{R_\mathrm{i}}v', \tag{13}$$

$$u'\frac{\partial V_\mathrm{i}}{\partial r'} \sim u'\frac{V_\mathrm{i}}{\Delta} \sim \nu\frac{\partial^2 v'}{\partial r'^2} \sim \nu\frac{v'}{\Delta^2}, \tag{14}$$

where V_i $(= At)$ is the speed of the inner cylinder. Here the boundary-layer thickness Δ has been used as a proper length scale in the radial direction. Relations (13) and (14) represent the balance between viscous and centrifugal forces and between inertial and viscous forces, respectively. Based on the above relations, the following relation is be obtained:

$$\frac{u'}{v'} \sim \frac{V_\mathrm{i}\Delta^2}{R_\mathrm{i}\nu} \sim \frac{\nu}{V_\mathrm{i}\Delta}. \tag{15}$$

From $u'/v' \sim (V_\mathrm{i}\Delta^2)/(R_\mathrm{i}\nu)$, $u = \nu u'/(Td)$ and $v = 2\nu v'/(Ad^2)$ the following relation between dimensionless amplitudes of u' and v' is yielded:

$$\frac{1}{v_0}\frac{u}{v} \sim \frac{\Delta^2}{d^2}\,(=\delta^2) \sim \tau, \tag{16}$$

where δ $(= \Delta/d \propto \sqrt{\tau})$ is the usual dimensionless boundary-layer thickness. It is noted that the radial velocity component u' is nondimensionalized by $\nu/(Td)$ instead of $\nu/(Ad^2)$ and the relation between the second and the third term in Eq. (15), i.e. $(V_\mathrm{i}\Delta^2)/(R_\mathrm{i}\nu) \sim \nu/(V_\mathrm{i}\Delta)$, the following interesting result is obtained:

$$T^* = \left(\frac{V_\mathrm{i}\Delta}{\nu}\right)^2\frac{\Delta}{R_\mathrm{i}} \sim \text{constant}. \tag{17}$$

Here T^* is the Taylor number based on the boundary-layer thickness. Now, the following relation is produced from the above relations:

$$T^* u^* \left(\frac{\partial v_0}{\partial r}\right) \sim v, \tag{18}$$

where $T^* = \tau^{7/2}T$ and $u^* = u/\tau$. For the case of $A \to 0$ the basic velocity profile finally becomes time-independent, i.e. $\tau_c \to \infty$, and Taylor vortices appear at $\tau_c^2 T > Ta_c$ [12]:

$$Ta_c = 1695 \quad \text{for } \eta \to 1. \tag{19}$$

Now, for small time we introduce a similarity variable $\zeta\ (= y/\tau^{1/2})$ and assume that dimensionless amplitude functions of disturbances have the forms of

$$\big[u(\tau,\zeta), v(\tau,\zeta)\big] = \big[\tau^{n+2}u^*(\zeta), \tau^n v^*(\zeta)\big], \tag{20}$$

which satisfy relation (16) since $v_0 \sim \tau$. This form, $u/v \sim \tau^2$, is quite different from those used in previous studies on impulsive spin-up and spin-down problems [8–10], where $v_0 \sim 1$ and $u/v \sim \tau$. To determine n in Eq. (20) we employ Shen's [13] momentary instability concept: the temporal growth rate of the kinetic energy of the perturbation velocity should exceed that of the basic velocity at the onset time of secondary motion. In the present system the dimensionless kinetic energy is defined as

$$E(t) = \frac{1}{2}\|\mathbf{u}^2\|, \tag{21}$$

where $\|\cdot\| = \frac{1}{\lambda}\int_0^{\lambda}\int_{R_i}^{R_o}(\cdot)r'\,\mathrm{d}r'\,\mathrm{d}z'$. Since there is no basic flow in the r'- and the z'-direction and the condition of $|u/v| \to 0$ is valid for $\tau \to 0$ (see the relation (16)), the dimensionless kinetic energy can be divided into the basic and the perturbed one:

$$E_0(\tau) = \frac{1}{2}\|v_0^2\|, \qquad E_1(\tau) = \frac{1}{2}\|v^2\|. \tag{22a,b}$$

Then the temporal growth rates of the basic kinetic energy $r_0(\tau)$ and the perturbation energy $r_1(\tau)$ are defined as the root-mean-squared quantities in the two-dimensional field:

$$r_0(\tau) = \frac{1}{\langle v_0\rangle}\frac{\mathrm{d}\langle v_0\rangle}{\mathrm{d}\tau}, \qquad r_1(\tau) = \frac{1}{\langle v_1\rangle}\frac{\mathrm{d}\langle v_1\rangle}{\mathrm{d}\tau}, \tag{23a,b}$$

where $\langle\cdot\rangle = \sqrt{\int_S(\cdot)^2\,\mathrm{d}S/S}$ and $S = \lambda(R_o - R_i)$ with $\mathrm{d}S = \lambda(R_o - R_i)\,\mathrm{d}\zeta$. For the case of $n = 1$ the condition of $r_0 = r_1$ is fulfilled at the onset time of $\tau = \tau_c$, which will be shown later. This means that the amplitude function v follows the behavior of v_0 for small τ, as shown in Eq. (6). A similar treatment can be found in problems of transient Bénard-type convection [14,15]. Furthermore the relation of $T^* \cong$ constant for large T is shown even in theoretical results from the amplification theory [4].

By the above reasoning we set $u = \tau^3 u^*(\zeta)$ and $v = \tau v^*(\zeta)$. For boundary-layer flow systems of $\delta \propto \sqrt{\tau}$, the dimensionless time τ plays dual roles of the boundary-layer thickness and time. Now, the self-similar stability equations are obtained in dimensionless form from Eqs. (11) and (12) as

$$\left[(D^2 - a^{*2})^2 + \frac{1}{2}(\zeta D^3 - 4D^2 - a^{*2}\zeta D + 3a^{*2})\right]u^* = v_0^* a^{*2} v^*, \tag{24}$$

$$\left(D^2 - a^{*2} + \frac{1}{2}\zeta D - 1\right)v^* = 2T^* D v_0^* u^*, \tag{25}$$

where $D = \mathrm{d}/\mathrm{d}\zeta$, $D^2 = \mathrm{d}^2/\mathrm{d}\zeta^2$, $y = \zeta\sqrt{\tau}$, $a^* = a\sqrt{\tau}$ and $v_0^* = v_0/\tau$. Here T^* and a^* have been treated as eigenvalues. The proper boundary conditions are

$$u^* = Du^* = v^* = 0 \quad \text{at } \zeta = 0 \quad \text{and } \zeta \to \infty. \tag{26}$$

Now, the minimum value of T^* should be found in the plot of T^* vs. a^* under the principle of the exchange of stabilities. In other words, the minimum value of τ, i.e. τ_c, and its corresponding wavenumber a_c should be obtained for a given T. Since time has been frozen by letting $\partial(\cdot)/\partial\tau \equiv 0$ under the frame of coordinates τ and ζ instead of τ and y, the propagation theory may be called the relaxed frozen-time model by treating τ as the parameter but it involves the time dependency implicitly.

2.3. Solution procedure

To find eigenvalues and eigenfunctions for differential equations, several methods such as the compound matrix and the shooting method have been proposed [16]. In the present study the stability equations (24)–(26) are solved by employing the latter method. In order to integrate these stability equations the proper values of D^2u^*, D^3u^* and Dv^* at $\zeta = 0$ are assumed for a given a^*. Since the stability equations and their boundary conditions are all homogeneous, the value of $D^2u^*(0)$ can be assigned arbitrarily and the value of the parameter T^* is assumed. This procedure can be understood easily by taking into account of the characteristics of eigenvalue problems [16]. After all the values at $\zeta = 0$ are provided, this eigenvalue problem can be proceeded numerically.

Integration is performed from $\zeta = 0$ to a fictitious upper boundary with the fourth order Runge–Kutta–Gill method. If the guessed values of T^*, $D^3u^*(0)$ and $Dv^*(0)$ are correct, u^*, Du^* and v^* will vanish at the upper boundary. Here, a relative error ε, defined as the absolute value of the difference between two successively calculated trial values divided by the former one, was chosen as a convergence criterion and convergence was assumed when $|\varepsilon| < 10^{-10}$. After the convergence was reached, the calculation depth ζ_f is increased by a fixed increment $\Delta\zeta_f$ and the incremental change in T^*, defined as

$$R \equiv \frac{T_n^* - T_{n+1}^*}{T_n^* \Delta\zeta_f} \tag{27}$$

was used as a convergence criterion for the calculated eigenvalue T^*. The maximum calculation depth $\zeta_{f,\max}$ and the required number of integration step n were determined so as that the incremental change R would not be lager than 10^{-4}. Near the marginal state the values of $\zeta_{f,\max} = 10$ and $n = 2000$ were used. Since disturbances decay exponentially outside the boundary-layer thickness, the incremental change R also decays exponentially with increasing a fictitious outer boundary thickness. This behavior enables us to extrapolate the eigenvalue T^* to the infinite depth by using the Shank transform [17].

The whole procedure is described in the work of Chen [18] and Kim [19]. A stability curve is shown in Fig. 3(a) and the minimun T^*-value is found to be 402.13 with its corresponding a^* value of 1.26.

3. Results and discussion

For the limiting case of $\tau \to 0$ the stability criteria of axisymmetric instability have been obtained from the propagation theory. The critical conditions from Fig. 3(a) can be converted into

$$\tau_c = 5.54T^{-2/7}, \quad a_c = 0.53T^{1/7} \quad \text{as } \tau \to 0. \tag{28a,b}$$

At this critical condition the profiles of amplitude functions are featured in Fig. 3(b). The critical time τ_c to mark the onset of a fastest growing instability decreases with increasing T. It is known that disturbances of the angular velocity are confined mainly within the hydrodynamic boundary layer of the primary flow (see Fig. 2). This means that the hydrodynamic boundary-layer thickness seems to be a proper length scale, which is the basic assumption in scale relations (13) and (14). The similar trend is also shown in Rayleigh–Bénard problems [20,21]. From distributions of the basic flow (Eq. (6)) and the perturbation quantities we can obtain the following equation:

$$r_0 = r_1 = \frac{5}{4\tau_c} \quad \text{as } \tau \to 0. \tag{29}$$

This verifies that the present propagation theory satisfies Shen's [13] momentary instability concept discussed in deriving Eqs. (24) and (25).

In Figs. 4 and 5 the above results are compared with Chen et al.'s [4] predictions and experimental data. Their acceleration procedure is slightly different from that of the present study. In their experiment the inner cylinder was accelerated with a constant acceleration rate A during the acceleration period of $0 \leqslant t \leqslant t_f$ and then kept at a constant velocity $V_f = At_f$:

$$V_0(R_i, t) = \begin{cases} At, & 0 \leqslant t \leqslant t_f, \\ V_f\ (= At_f), & t > t_f. \end{cases} \tag{30}$$

Flow characteristics were visualized injecting dye solution into the flow field and recorded using a high-speed movie camera. The detection time of secondary motion t_o and the average vortex wavelength λ_c were determined by examining the recorded film. When $t_f \leqslant t_o$, secondary motion is observed during the constant acceleration period and the present constant acceleration model can be applied. For the other limiting case of $t_f \ll t_c$ secondary motion sets in after the constant acceleration period and the impulsive acceleration model [8] can be applied with a certain time delay due to the finite acceleration. For the intermediate region of $t_c \leqslant t_f \leqslant t_o$ the present prediction may be used as the first approximation.

Chen et al. [4] analyzed their experimental situation of Eq. (30) by employing the amplification theory, where for a given wavelength the time evolution of the volume-integrated kinetic energy of disturbances assumed arbitrarily at $t = 0$ was monitored. They suggested the intrinsic characteristic time t_i, up to which the kinetic energy of a most dangerous mode of disturbances should decay. They reported that the secondary flow pattern became clearly observable when the rms-values of their initial disturbance kinetic energy at $t = 0$ increased 10^3-fold at $t = t_3$, i.e. $E_1(\tau_3)/E_1(0) = 10^3$ at $\tau = \tau_3$ (see Eq. (22b)). Fig. 4 illustrates that the present predictions of $\tau_o \cong 2\tau_c$ for $\tau \to 0$ compare well with their experimental and theoretical results for the case of $\eta = 0.2$. The present τ_c-value from Eq. (28a) agrees well with their intrinsic one τ_i from the amplification theory. The present critical wavenumbers are comparable with their theoretical and experimental ones, as shown in Fig. 5. Their flow visualization results show that the disk-like cell spacing (wavelength) is almost constant during $t_c \leqslant t \leqslant t_o$ ($\cong 2t_c$) and even

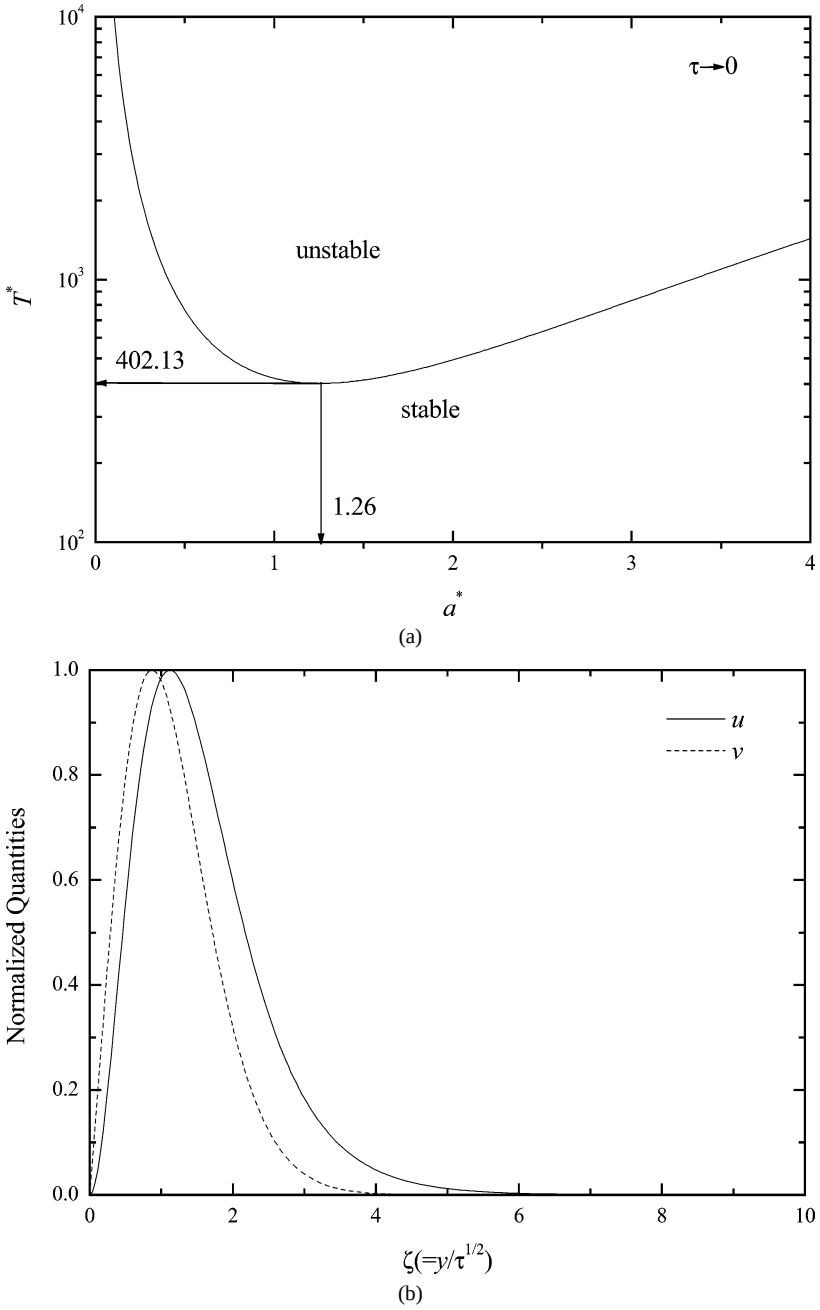

Fig. 3. Instability conditions for small time of $\tau_c \to 0$ from the propagation theory: (a) marginal stability curve and (b) amplitude profiles at $\tau = \tau_c$.

after first detection time of secondary motion, t_o. These disk-like cells develop into Taylor–Görtler vortices. It is very interesting that the present predictions agree very well with those from the amplification theory. For transient instability problems on thermal convection Foster [22] commented that with correct dimensional relations the relation of $\tau_o \cong 4\tau_c$ would be kept for the case of impulsive heating in horizontal fluid layers which corresponds to that of impulsive spin-up or spin-down. For latter case the same relation of $\tau_o \cong 4\tau_c$ has been reported based on the amplification theory [5] and also the propagation theory [8–10]. However, the relation of $\tau_o \cong 2\tau_c$ was suggested based on the amplification theory for the constant acceleration problem [4] and also based on the propagation theory for the ramp heating case of Rayleigh–Bénard convection [23]. All the above results imply that the predicted critical time t_c is smaller than the detection time t_o, i.e. a fastest growing mode of instabilities, which

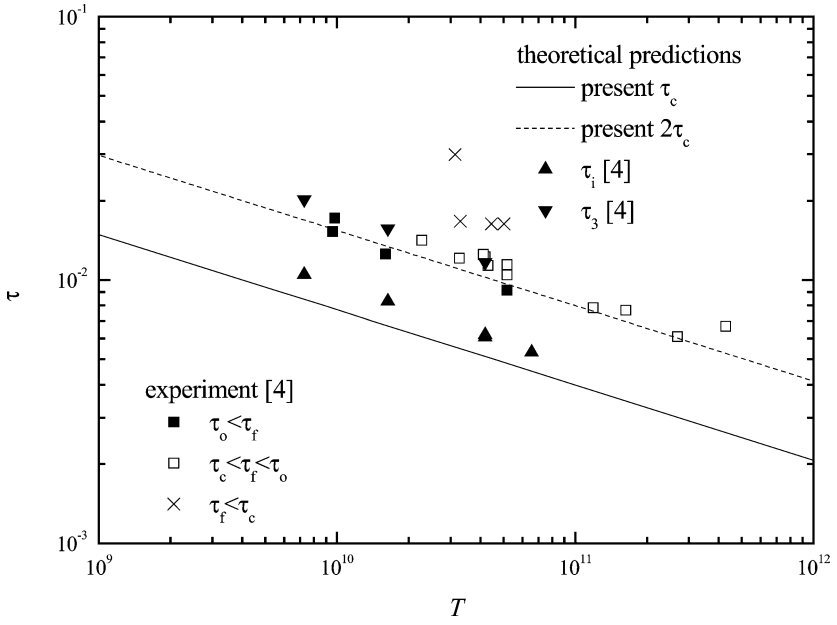

Fig. 4. Comparison of present characteristic times with Chen et al.'s [4] predictions and experimental data for $\eta = 0.2$.

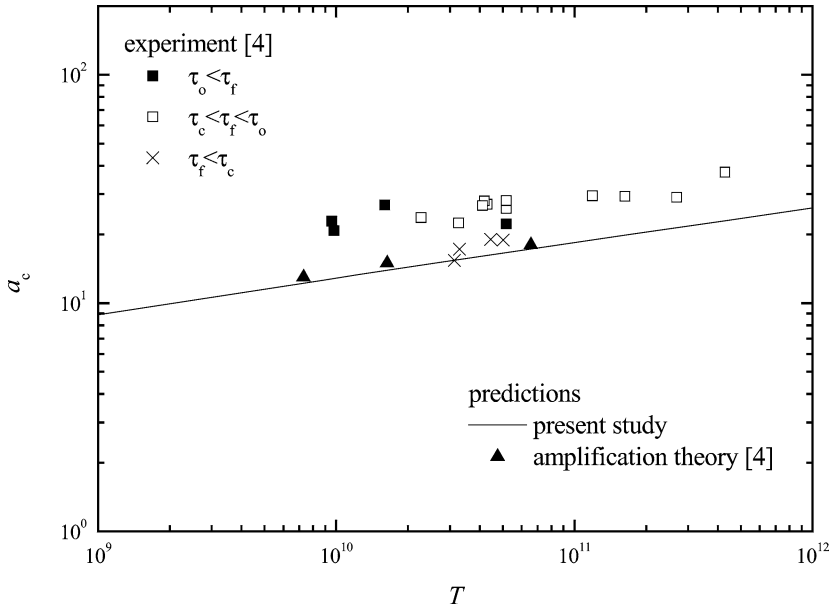

Fig. 5. Comparison of the present critical wavenumber a_c with Chen et al.'s [4] predictions and experimental data for $\eta = 0.2$.

sets in at $t = t_c$, will grow with time until manifest motion is first detected experimentally. This growth period depends on the acceleration or heating history. To find out the growing mechanism and the effect of acceleration history on the critical conditions, a more refined analysis is now in progress by assuming some initial conditions and following the procedure and concept in Choi et al.'s [24] work on Rayleigh–Bénard convection.

It is known that the propagation theory, which is based on the self-similar transformation and normal mode analysis, is a powerful method to predict the stability criteria reasonably well in simple hydrodynamic or thermal systems.

4. Conclusion

The onset of a fastest growing, axisymmetric instability in Couette flow induced by a linearly accelerated inner cylinder has been investigated by the propagation theory, which was originally developed for the analysis of thermal instabilities leading to Bénard-like convection. The dimensionless critical time τ_c to mark the onset of a fastest growing instability has been obtained as a function of the modified Taylor number T. The present predictions of instability criteria on axisymmetric flow bound available experimental data, which are the almost the same as those from the amplification theory. The relation of $\tau_o \cong 2\tau_c$ represents the characteristic time of first detection of manifest secondary motion to a certain degree in the present system.

Acknowledgements

This work was supported by a grant form the Chuongbong Academic Research Fund of the Cheju National University Development Foundation.

References

[1] P.M. Schweizer, L.E. Scriven, Evidence of Görtler-type vortices in curved film flows, Phys. Fluids 26 (1983) 619–623.
[2] A. Yeckel, J.J. Derby, Effect of accelerated crucible rotating on melt composition in high pressure vertical Bridgman growth of cadmium zinc telluride, J. Crystal Growth 209 (2000) 734–750.
[3] C.F. Chen, D.K. Christensen, Stability of flow induced by an impulsively started rotating cylinder, Phys. Fluids 10 (1967) 1845–1846.
[4] C.F. Chen, D.C.S. Liu, M.W. Skok, Stability of circular Couette flow with constant finite acceleration, Trans. ASME J. Appl. Mech. 40 (1973) 347–354.
[5] C.F. Chen, B.P. Kirchner, Stability of time-dependent rotational Couette flow. Part 2. Stability analysis, J. Fluid Mech. 48 (1971) 365–384.
[6] G.P. Neitzel, Stability of circular Couette flow with variable inner cylinder speed, J. Fluid Mech. 123 (1982) 43–57.
[7] K.-K. Tan, R.B. Thorpe, Transient instability of flow induced by an impulsively started rotating cylinder, Chem. Eng. Sci. 58 (2003) 149–156.
[8] M.C. Kim, T.J. Chung, C.K. Choi, The onset of Taylor-like vortices in the flow induced by an impulsively started rotating cylinder, Theoret. Comput. Fluid Dynamics 18 (2004) 105–114.
[9] M.C. Kim, C.K. Choi, The onset of instability induced by an impulsively started rotating cylinder, Chem. Eng. Sci. 60 (2005) 599–608.
[10] M.C. Kim, C.K. Choi, The onset of Taylor–Görtler vortices in impulsively decelerating swirl flow, Korean J. Chem. Eng. 21 (2004) 767–772.
[11] S.O. MacKerrell, P.J. Blennerhassett, P. Bassom, Görtler vortices in the Rayleigh layer on an impulsive started cylinder, Phys. Fluids 14 (2002) 2948–2956.
[12] S. Chandrasekhar, Hydrodynamic and Hydromagnetic Stability, Oxford University Press, Oxford, 1961.
[13] S.F. Shen, Some considerations on the laminar stability of time-dependent basic flows, J. Aero. Sci. 28 (1961) 397–417.
[14] C.K. Choi, K.H. Kang, M.C. Kim, I.G. Hwang, Convective instabilities and transport properties in horizontal fluid layers, Korean J. Chem. Eng. 15 (1988) 192–198.
[15] K.H. Kang, C.K. Choi, I.G. Hwang, Onset of solutal Marangoni convection in a suddenly desorbing liquid layer, AIChE J. 46 (2000) 15–23.
[16] B. Straughan, The Energy Method, Stability, and Nonlinear Convection, Springer-Verlag, NY, 1992.
[17] O.T. Hanna, O.C. Sandall, Computational Method in Chemical Engineering, Prentice-Hall, NJ, 1995.
[18] K. Chen, Thermal instability of wedge Flows, Ph.D. thesis, University of Illinois, Urbana-Champaign, IL, 1981.
[19] M.C. Kim, The onset of natural convection and heat transfer correlations in systems experiencing thermal boundary layer characteristics, Ph.D. thesis, Seoul National University, Seoul, Korea, 1992.
[20] D.J. Yang, C.K. Choi, The onset of thermal convection in a horizontal fluid layer heated from below with time-dependent heat flux, Phys. Fluids 14 (2002) 930–937.
[21] M.C. Kim, H.K. Park, C.K. Choi, Stability of an initially, stably stratified fluid subjected to a step change in temperature, Theoret. Comput. Fluid Dynamics 16 (2002) 49–57.
[22] T.D. Foster, Onset of manifest convection in a layer of fluid with a time-dependent surface temperature, Phys. Fluids 12 (1969) 2482–2487.
[23] M.C. Kim, T.J. Chung, C.K. Choi, Onset of buoyancy-driven convection in the horizontal fluid layer heated from below with time-dependent manner, Korean J. Chem. Eng. 21 (2004) 69–74.
[24] C.K. Choi, J.H. Park, H.K. Park, H.J. Cho, T.J. Chung, M.C. Kim, Temporal evolution of thermal convection in an initially, stably stratified fluid, Int. J. Therm. Sci. 43 (2004) 817–823.